Structural Characteristics and Optical Properties of Thermally Oxidized Zinc Films

D.I. Rusu*, G.G. Rusu and D. Luca

Faculty of Physics, "Al. I. Cuza" University, 11 Carol I Blvd., 700506 Iasi, Romania

(Received October 24, 2010; revised version February 10, 2011; in final form March 10, 2011)

Zinc oxide (ZnO) thin films (with thickness ranged from 780 nm to 1150 nm) were prepared by thermal oxidation in air (at 600–700 K, for 20–30 min) of vacuum evaporated metallic zinc films. The Zn films were deposited on glass substrates at room temperature. The crystalline structure of ZnO thin film samples was investigated using X-ray diffraction technique. The diffraction patterns revealed that the ZnO thin films were polycrystalline and have a wurtzite (hexagonal) structure. The film crystallites are preferentially oriented with (002) planes parallel to substrate surface. Some important structural parameters (lattice parameters of the hexagonal cell, crystallite size, Zn–O bond length, residual stress, etc.) of the films were determined. The surface morphology of the prepared ZnO thin films, investigated by atomic force microscopy, revealed a uniform columnar structure. The spectral dependence of transmission coefficient has been studied in the wavelength range from 300 nm to 1700 nm. The optical energy band gap calculated from the absorption spectra (supposing allowed direct band-to-band transitions) are in the range 3.17–3.19 eV. The dependence of the microstructural and optical characteristics on the preparation conditions (oxidation temperature, oxidation time, etc.) of the oxidized zinc films is discussed.

PACS: 77.55.hf, 68.55.−a, 68.55.J−, 81.15.Aa, 78.20.−e

1. Introduction

Due to their wide direct optical band gap (about 3.37 eV at room temperature), high transmission coefficient ($> 80\%$) in the visible and near infrared spectral range, high electrical conductivity, important piezoelectric and photoelectric properties (e.g. large exciton binding energy of 60 meV at 300 K) [1–8], zinc oxide (ZnO) thin films and nanostructures have an increasing role in modern solid state device technology (transparent field effect transistors, light emitting diodes, gas sensors, solar cells, transparent conducting electrodes, electronics in ultraviolet and blue spectral ranges, etc.) [1, 2, 9–13].

A significant progress in the preparation technology of films and heterostructures based on ZnO has been observed in the last years [1, 5–8].

Many techniques have been used in order to prepare high-quality ZnO thin films, including magnetron sputtering, molecular beam epitaxy, pulsed laser deposition, spray pyrolysis, spin coating, chemical vapor deposition, etc. [3–6, 14–17].

Few information relating to ZnO thin films prepared by thermal oxidation of metallic zinc films are reported in literature [5–8]. Thermal dry oxidation (oxidation in oxygen ambient) is the most frequently used method of oxide formation during this process. It is however well known that structural, electronic transport and optical properties of ZnO thin films strongly depend both on structural characteristics of metallic zinc films (which, in their turn, depend on the deposition parameters) and on the oxidation conditions (oxidation temperature, heating rate, oxidation time, etc.).

It was shown that the use of thermal oxidation of zinc films for producing ZnO thin films is recommended because this is low-cost method which provides the possibility of obtaining stoichiometric and homogeneous films, doped films and ZnO films with large thickness.

An important number of experimental results are, at present, obtained by using thin films with lower thicknesses (usually, less than 200 nm). As compared with other methods, the oxidation of the metallic zinc films has some important advantages: simplified deposition process, the possibility of controlling structural characteristics, processing of multilayered structures, etc. [5–7].

In the present paper we report on the structural and optical characteristics of the ZnO thin films prepared by thermal oxidation in air of metallic zinc films. Some correlations between the film structure, optical properties of ZnO films and their preparation conditions were established.

2. Experimental

Metallic zinc thin films were deposited onto glass (Corning 2947) substrates by thermal evaporation under vacuum (using the quasi-closed volume technique [18]). The material for evaporation was metallic zinc powder having a purity of 99.993%. Zinc oxide thin films were prepared by thermal oxidation (in open atmosphere at relative humidity about 60%) of as-deposited zinc metallic thin films.

Before deposition, the substrates were cleaned with chromic acid, ethanol and double-distilled deionized water. Finally, they were dried in vacuum at temperature

* corresponding author; e-mail: d_i_rusu@yahoo.com

of 600 K for 1 h. More details on the deposition equipment have been described in detail in our previous papers [7, 18, 19].

The following values of deposition parameters were used: evaporator (source)–substrate distance, d_{es} = 8 cm; source temperature, $T_{ev} = 700$ K; deposition rate, r_d = 13–14 Å/s; substrate temperature, T_s = 300 K. These parameters are kept constant during the deposition for all zinc films referred in this paper.

The oxidation process consisted of the three successive technological steps: (i) heating of zinc films from room temperature to the oxidation temperature, T_0 (T_0 was varied between 600 and 700 K, with increasing temperature rate of 6–8 K/min); (ii) annealing for a certain oxidation time τ_0 (τ_0 = 20–30 min) at oxidation temperature, T_0; (iii) cooling down from the oxidation temperature to room temperature with a temperature decreasing rate of 10–15 K/min. These oxidation conditions permit to prepare ZnO thin films with stable structure, stoichiometric and homogeneous composition and with good adhesion to the substrate.

The thickness of ZnO thin films (which ranged between 780 nm and 1150 nm), was determined by an interferometric method (multiple-beam Fizeau's fringe method [13] by the reflection of a monochromatic light-beam with $\lambda = 550$ nm).

The crystalline structure of ZnO films was analysed by X-ray diffraction (XRD) technique, using Cu K_α radiation (λ = 1.5418 Å) in the 2θ range from 20° to 90° [20, 21].

The surface microstructure of the films was examined by an *ex situ* atomic force microscopy (AFM). The AFM images were acquired in the tapping mode and in the repulsive force regime.

The optical reflection and transmission coefficients were recorded at room temperature, within the wavelength range from 300 nm to 1700 nm using a TEC-5 computer controlled spectrometer.

The absorption coefficient, α_λ, was determined from the expression [22, 23]

$$\alpha_\lambda = \frac{1}{d} \ln \frac{(1 - R_\lambda)^2}{T_\lambda}, \tag{1}$$

where d denotes the film thickness, T_λ and R_λ are the transmission and reflection coefficients at wavelength λ, respectively.

3. Results and discussion

3.1. Microstructural characteristics

The XRD patterns were used for identification of crystalline phases and microstructural analysis of the prepared ZnO thin films. Figures 1 and 2 show the representative XRD patterns.

In order to establish the influence of the structural characteristics of vacuum evaporated Zn thin films on the structure of ZnO thin films, the following experimental procedure was used: in the similar deposition conditions, two series of thin-film samples were obtained. The structure of first series was investigated by XRD technique immediately after deposition and the second series was submitted to a thermal oxidation (oxidation conditions were presented in Table I) and then was studied by XRD analysis.

TABLE I

Oxidation conditions and values of texture coefficient for ZnO thin films.

Sample	d [nm]	T_0 [K]	τ_0 [min]	$TC(hkl)$ [%]		
				(100)	(002)	(101)
OXZ.60.07	780	600	20	0.23	2.49	0.56
OXZ.60.09	900	600	20	1.35	2.03	1.08
OXZ.70.10	1020	700	30	1.23	2.38	1.19
OXZ.70.11	1150	700	30	1.47	2.16	1.30

d, film thickness; T_0, oxidation (annealing) temperature; τ_0, oxidation time; $TC(hkl)$, texture coefficient for (hkl) peaks

The typical XRD patterns are shown in Figs. 1 and 2. It can be observed from Fig. 1a that zinc films are polycrystalline and have a hexagonal close-packed structure. The reflection corresponding to the (002) planes become more evidenced. Therefore, the films crystallites are preferentially oriented with c-axis normal to substrate surface.

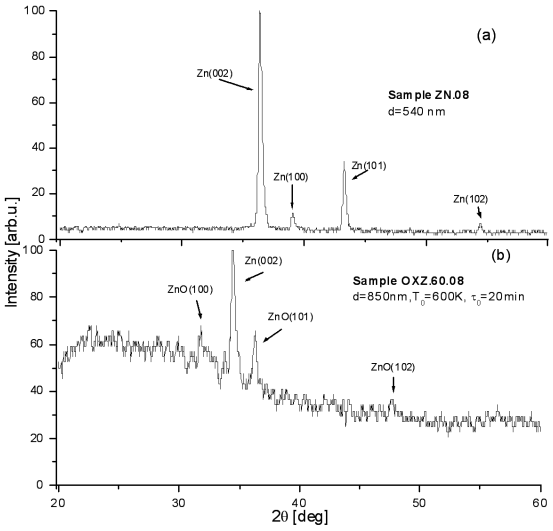

Fig. 1. XRD patterns for two investigated samples: (a) sample ZN.08 as-deposited zinc film (b) sample OXZ.60.08 oxidized at temperature T_0 = 600 K for τ_0 = 20 min.

Figure 2 presents XRD patterns for four ZnO films with different thickness, thermally oxidized in various conditions. The indexed diffraction peaks were used to calculate the interplanar spacings corresponding to the (100), (002) and (101) planes of the hexagonal (wurtzite)

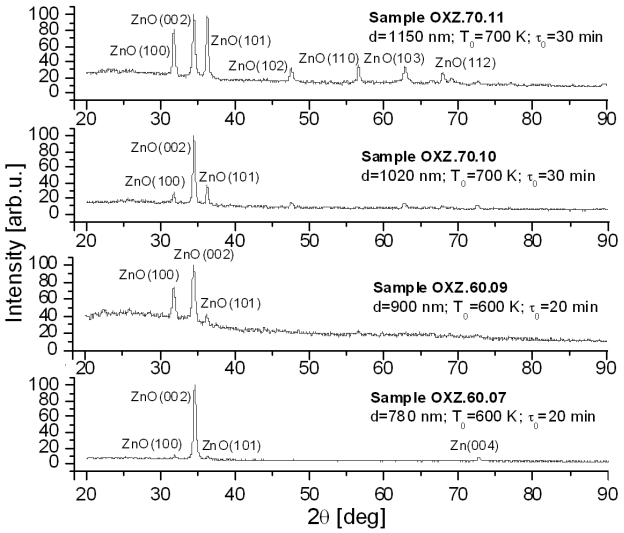

Fig. 2. The X-ray diffraction patterns of ZnO thin films with different thickness.

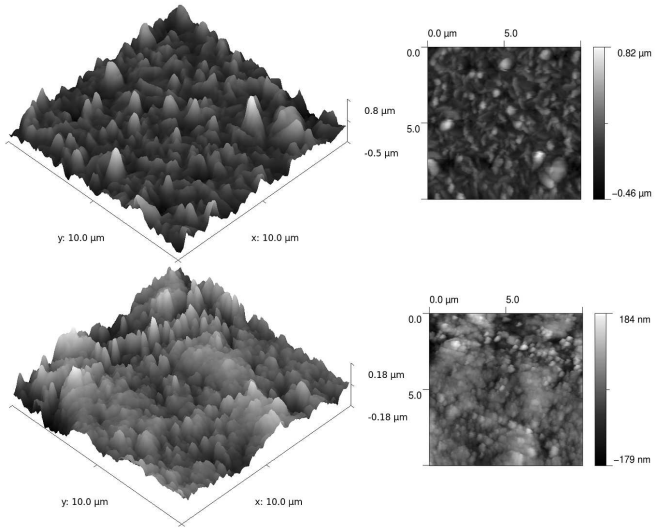

Fig. 3. AFM images (3D and 2D) for ZnO thin films with different thickness: (a) sample OXZ.60.07 (d = 780 nm; T_0 = 600 K; t_0 = 20 min; R_a = 108 nm; R_rms = 144 nm); (b) sample OXZ.70.11 (d = 1150 nm; T_0 = 700 K; t_0 = 30 min; R_a = 35 nm; R_rms = 45 nm).

ZnO crystalline structure [1, 11, 14–16]. It can be observed that the diffraction patterns do not indicate the presence of zinc crystalline phase in ZnO films. Therefore, the used oxidation conditions provide growth of nearly stoichiometric ZnO films, having a single phase of ZnO.

Structural investigations showed that the zinc oxide films prepared under the mentioned conditions are polycrystalline and have a wurtzite (hexagonal) structure [2–4]. For all ZnO films, crystallites are preferentially oriented with (002) planes parallel to the substrate surface. The c-axis of hexagonal cell is normal to substrate, resulting in columnar crystallites that are perpendicular to the substrate surface (this structure is confirmed by AFM images in Fig. 3). The (100) and (101) planes are also evidenced in the XRD patterns.

TABLE II

Structural characteristics of zinc films and zinc oxide films.

Sample	d [nm]	T_0 [K]	τ_0 [min]	2θ [degree]	(hkl)	a [Å]	c [Å]
ZN.08	540	–	–	36.28	002	–	4.946
				39.00	100	2.664	–
OXZ.60.08	850	600	20	31.75	100	3.236	–
				34.35	002	–	5.218

d, film thickness; T_0, oxidation temperature; τ_0, oxidation time; θ, Bragg angle; (hkl), Miller indices; a and c, lattice parameters of the hexagonal (wurtzite) structure

Lattice parameters of ZnO wurtzite structure, a and c, were calculated using a well-known analytical method [20]. Some structural characteristics of zinc film and zinc oxide film for one of our samples are shown in Table II. The obtained results for other samples are presented in Table III. For the ZnO films oxidized at higher temperature, these values, calculated using the (002) and (100) diffraction peaks, are slightly larger than standard values for ZnO polycrystalline powder (a = 3.249 Å, c = 5.201 Å) [14, 16]. This fact can be explained as an effect of the oxygen depletion in the film during oxidation process [14, 16]. The presence of other phases in ZnO system, as well of non-oxidized Zn atoms is not observed.

For the ZnO films obtained at lower oxidation temperature, the values of c-parameter of hexagonal cell (around 5.193 Å), calculated from the (002) peak position are very close to the c-parameter values of the bulk ZnO crystals [2, 24], indicating that the films are displaying a low degree distortion due to the structural defects at film–substrate interface.

The average crystallite size were calculated from the Debye–Scherrer formula [20, 24]

$$D = \frac{k\lambda}{\beta_{2\theta}\cos\theta}\,, \tag{2}$$

where k denotes the Scherrer constant (the shape factor of the average crystallite and can be considered $k = 0.90$ [25, 26]); λ = 1.5418 nm is the wavelength of the incident Cu K_α radiation; $\beta_{2\theta}$ represents the full-width at half-maximum of the respective peak and θ is the Bragg diffraction angle.

For some studied samples, the crystallite sizes, calculated from Eq. (2) are presented in Table III. The average size varied from 24.68 nm to 32.21 nm. The films with greater thickness are characterized by greater crystallite size.

The Zn–O bond length, L, was also calculated using the relation [26, 27]:

$$L = \left[\frac{a^2}{3} + \left(\frac{1}{2} - u\right)^2 c^2\right], \tag{3}$$

where the u parameter for wurtzite structure can be expressed as [27]:

$$u = \frac{a^2}{3c^2} + 0.25\,. \tag{4}$$

The values obtained for the bond length are indicated in Table III. It is known that ionic radius of O^{2-} is 1.38 Å [26] and ionic radius of the Zn^{2+} is 0.83 Å [2]. Consequently, the length of the Zn–O bond is 2.21 Å. The small values obtained for our samples indicate the presence of the structural defects (especially, oxygen vacancies).

TABLE III

Structural parameters of the investigated ZnO thin films.

Sample	d [nm]	r_d [Å/s]	T_s [K]	T_0 [K]	τ_0 [min]	2θ [degree]	(hkl)	d_{hkl} [Å]	a [Å]	c [Å]
OXZ.60.07	780	15	300	600	20	34.4	002	2.604	–	5.193
OXZ.60.09	900	14	300	600	20	31.7	100	2.803	3.241	–
						34.4	002	2.592	–	5.192
OXZ.70.10	1020	13	300	700	30	31.7	100	2.816	3.266	–
						34.4	002	2.603	–	5.208
OXZ.70.11	1150	14	300	700	30	31.7	100	2.808	3.247	–
						34.4	002	2.607	–	5.204

d, film thickness; r_d, deposition rate; T_s, substrate temperature; T_0, oxidation temperature; τ_0, oxidation time; θ, Bragg angle; (hkl), Miller indices; d_{hkl}, interplanar spacing of (hkl) planes; a and c, lattice parameters of the hexagonal (wurtzite) structure

TABLE IV

The values of some structural parameters of the studied ZnO thin films.

Sample	d [nm]	T_0 [K]	τ_0 [min]	D [nm]			c/a (002)	L [nm]	d_c [nm]
				(002)	(100)	(101)			
OXZ.60.07	780	600	20	26.23	–	–	1.60	1.94	3.18
OXZ.60.09	900	600	20	30.93	28.41	28.46	1.61	1.93	3.18
OXZ.70.10	1020	700	30	27.97	24.68	26.97	1.60	1.94	3.19
OXZ.70.11	1150	700	30	32.21	27.68	27.37	1.61	1.93	3.18

d, film thickness; T_0, oxidation temperature; τ_0, oxidation time; D, crystallite size (calculated taken into account indicated peaks of the wurtzite structure); c/a, ratio of lattice parameters; L, length of Zn–O bond; d_c, cation–cation distance

It is known that cation–cation distance for wurtzite structure [28, 29] is

$$d_c = cx\left(\frac{3}{8}\right)^{1/2}, \tag{5}$$

where c is parameter of hexagonal (wurtzite) cell (the height of hexagonal prism).

For our samples, the obtained values of d_c are lower than those reported for bulk ZnO crystals [29].

The preferred orientation of particular crystal planes relative to film substrate can be quantitatively evaluated using texture coefficient, $TC(hkl)$, which has been determined from expression [30, 31]:

$$TC(hkl) = \frac{I(hkl)/I_0(hkl)}{(1/n)\sum_n I(hkl)/I_0(hkl)}\,, \tag{6}$$

where $I(hkl)$ is intensity of the XRD peak corresponding to (hkl) planes, n is the number of the diffraction peaks taking into account, $I_0(hkl)$ denotes the intensity of the XRD peak reference of the randomly oriented crystallites. For some studied samples, the $TC(hkl)$ values for (002), (101) and (100) planes are listed in Table I, together with the oxidation conditions.

It can be observed that $TC(002)$ is greater than 2 for all samples. According to Eq. (6) if $TC(hkl)$ is equal to one for all the considered (hkl) planes, then the films are characterized by a randomly crystallite orientation, similar to the standard (reference) JCPDS XRD pattern [21]. $TC(hkl)$ values higher than one show that a large number

of crystallites are oriented with their (hkl) planes parallel to substrate surface.

Table I also shows that film crystallites preferentially oriented with c-axis of hexagonal cell normal to the substrate surface are characterized by larger size. This behavior can be explained by supposing that these crystallites are present in early stages of film growth. It can be observed from XRD patterns (Fig. 2) that the films with lower thickness have a high intensity (002) peak. The $TC(hkl)$ values decrease with increasing oxidation temperature.

The texture coefficient depends on the film thickness. At smaller thickness, film crystallites are preferentially oriented with their c-axis perpendicular to the substrate surface. We observe that an increase of the oxidation time results in increase of the crystallite size.

The standard value of the c/a ratio for the wurtzite structure is about 1.63. There is a good agreement between obtained values (Table III) and standard one. Therefore, it can be supposed that crystallites, preferentially oriented with (002), (110) and (101) parallel to the substrate surface, have a crystalline structure with small concentration of structural defects [2, 9].

Additional information on the structural characteristics of studied films can be obtained from the calculation of strain and residual stress.

The strain in ZnO thin films along c-axis perpendicular to substrate surface can be calculated using the following expression [31]:

$$\varepsilon_2[\%] = \frac{c - c_0}{c_0} \times 100\,, \tag{7}$$

where c denotes the lattice parameter of hexagonal (wurtzite) cell of the ZnO films, c_0 is the unstrained lattice parameter for bulk ZnO ($c_0 = 5.2066$ Å [24]).

The residual stress, σ, in ZnO thin film can be determined by relationship [32]:

$$\sigma = \frac{2c_{13}^2 - c_{33}\,(c_{11} + c_{12})}{2c_{13}} \frac{c - c_0}{c_0}\,, \tag{8}$$

where c_{ij} represent elastic stiffness constants for ZnO single crystals; $c_{11} = 208.8$ GPa, $c_{33} = 213.8$ GPa, $c_{12} = 119.7$ GPa, and $c_{13} = 104.2$ GPa [27].

Using indicated values for c_{ij} coefficients of the residual stress value can be estimated from [29]:

$$\sigma = -232.8 \frac{c - c_0}{c_0}\ [\text{GPa}]\,. \tag{9}$$

The c-parameter values and the calculated stress, using Eq. (9), for some studied samples are indicated in Table IV.

The residual stress of samples OXZ.60.07 and OXZ.60.09 is tensile and for samples OXZ.70.10 and OXZ.70.11 is compressive. Consequently, the annealing at 700 K determines the elimination of tensile film stress and improves film crystallinity (as also the XRD studies confirm).

The surface microstructure of the films was investigated by an *ex situ* atomic force microscopy (AFM). The AFM images depicted in Fig. 3 show that the film microstructure is characterized by high-density columnar structure with low surface roughness. It can be observed that by increasing film thickness the crystallites are getting larger and begin to agglomerate and to form clusters. The average roughness, R_a, was calculated by expression

$$R_a = (1/N) \sum_{i=1}^{N} |z_m - z_i|\,, \tag{10}$$

where N is the number of deviations in height (z_i) from the profile mean value (z_m).

The average surface roughness, R_a, varied between 35 nm and 108 nm, depending on film thickness. The AFM images show the differences between the surfaces roughness of the films oxidized at different temperatures.

AFM images show that the films are grain-like and crystallite size increases with increasing film thickness.

The obtained results for two studied samples are shown in Fig. 3. It is noted from these images that in the film annealed at 600 K the crystallite size becomes much broader than these annealed at 700 K. This is in good agreement with crystallite size determined by the Debye–Scherrer expression (Table III).

TABLE V

Values of strain and residual stress for some studied samples.

Sample	d [nm]	T_0 [K]	τ_0 [min]	c [Å]	$\varepsilon \times 10^{-3}$ [%]	σ [GPa]
OXZ.60.07	780	600	20	5.193	−2.6	0.605
OXZ.60.09	900	600	20	5.192	−2.8	0.651
OXZ.70.10	1020	700	30	5.208	2.6	−0.605
OXZ.70.11	1100	700	30	5.204	−0.4	0.093

d, film thickness; T_0, oxidation temperature; τ_0, oxidation time; c, lattice parameter of the hexagonal (wurtzite) structure; ε, strain along c-axis; σ, residual stress

3.2. Optical characteristics

The typical optical transmission spectra of two investigated ZnO thin film samples in the wavelength range between 300 nm and 1800 nm are presented in Fig. 4.

It is known that optical transmission of the thin films depends on the thickness and the surface morphology of the respective films. Generally, as the film is thinner and its surface morphology is more uniform, the transmission coefficient of the film becomes higher.

The average transmittance in the domain from 700 to 1600 nm of spectra was ranged between 80% and 90% for all studied samples. With increasing film thickness, the transmission coefficient decreases, due to the thickness effect [22].

It can be observed from Fig. 4 that transmission spectra present a sharp edge at a wavelength corresponding to the forbidden energy gap of ZnO crystals [2, 9, 13, 22]. This behavior shows that the studied films have a stoichiometric and homogeneous structure [11, 30]. With increase of the oxidation time, the transmission edge becomes sharper, indicating an improvement in the crystalline structure of the films. It was also established that

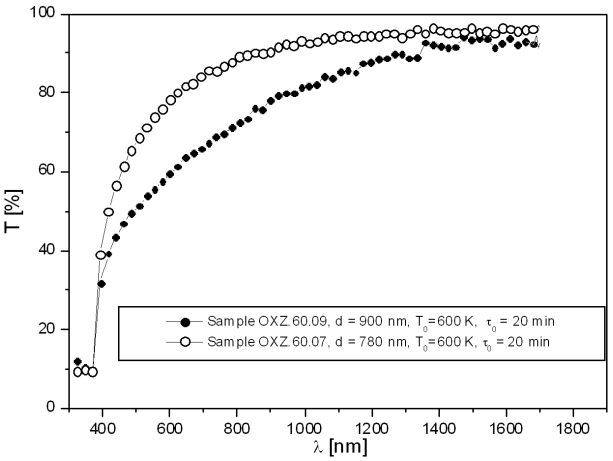

Fig. 4. Typical transmission spectra for ZnO thin films (samples OXZ.60.07 and OXZ.60.09).

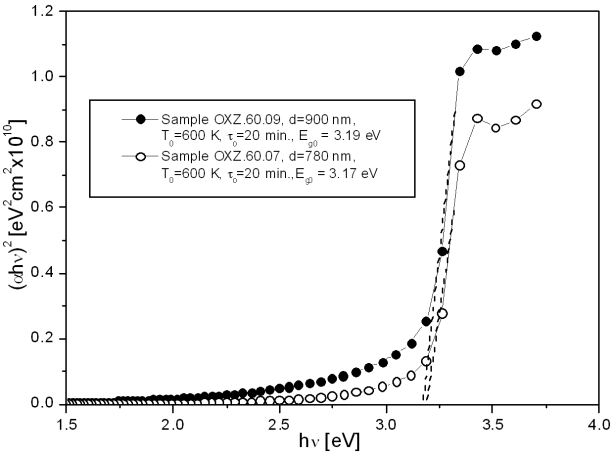

Fig. 5. The plots of $(\alpha h\nu)^2$ vs. photon energy, $h\nu$, for two ZnO thin films (samples OXZ.60.07 and OXZ.60.09).

the increase of the oxidation time results in an important decrease of the transmission coefficient.

The absorption coefficient was calculated taking into account Eq. (1). It is well known that investigation of the fundamental absorption edge of the semiconducting thin films provides important information on the characteristics of interband electronic transitions and the value of optical energy bandgap [13, 22].

Near the absorption edge, the energy dependence of the absorption coefficient, α, can be described by the following expressions proposed by Tauc [9, 28]:

— for the allowed direct transitions (neglecting exciton effect)

$$\alpha h\nu = A_{\mathrm{d}} \left(h\nu - E_{\mathrm{g0}}\right)^{1/2}; \tag{11}$$

— for the forbidden direct transitions (also neglecting exciton effect)

$$\alpha h\nu = A_{\mathrm{i}} \left(h\nu - E_{\mathrm{g0}}\right)^{3/2}. \tag{12}$$

In Eqs. (11) and (12), $h\nu$ is incident photon energy, E_{g0} denotes the optical energy band gap (for wave vector $\boldsymbol{k} = 0$), and A_{d} and A_{i} are characteristic parameters (independent of photon energy) for respective transitions [22].

ZnO crystals are characterized by direct optical transitions [2–4]. Consequently, according to Eq. (11), in the vicinity of the fundamental (intrinsic) absorption edge $(\alpha h\nu)^2$ linearly depends upon the photon energy $h\nu$. Thus, by extrapolating the linear portions of the $(\alpha h\nu)^2 = f(h\nu)$ dependences to $(\alpha h\nu)^2 \to 0$ one can determine the value of E_{g0} for direct transitions. These dependences are presented in Fig. 5. The obtained values of the band-gap width, E_{g0}, ranged between 3.17 eV and 3.19 eV. These values are in good agreement with those reported for bulk ZnO samples [2, 7, 33, 34].

4. Conclusions

It was found that polycrystalline ZnO thin films with high transmission coefficient (80%–90% in visible spectral range) and hexagonal (wurtzite) structure, highly oriented with *c*-axis perpendicular to the substrate surface, can be prepared by thermal oxidation of vacuum evaporated zinc metallic films.

The film thickness was varied in the range from 780 nm to 1150 nm.

The structural characteristics (crystallite size, Zn–O bond length, texture coefficient, strain, etc.) of the films studied by XRD, AFM and X-ray photoelectron spectroscopy (XPS) show a good crystallinity columnar growth and a smooth surface.

In the wavelength range from 600 nm to 1600 nm, the transmission coefficient is generally over 80%. The optical band-gap energy calculated from absorption spectra (considering allowed direct transitions) were in the range 3.17–3.19 eV.

References

[1] H.L. Hartnagel, A.L. Dawar, A.K. Jain, C. Jagadish, *Semiconducting Transparent Thin Films*, Institute of Physics Publishing, Bristol 1995.

[2] *Polycrystalline Semiconductors: Physical Properties and Applications*, Ed. G. Harbeke, Springer-Verlag, Berlin 1985.

[3] W.L. Dang, Y.Q. Fu, J.K. Luo, A.J. Flewitt, W.I. Milne, *Superlattices Microstruct.* **42**, 89 (2007).

[4] *Zinc Oxide Bulk, Thin Films and Nanostructures Processing, Properties and Applications*, Eds. C. Jagadiste, S.Y. Pearson, Elsevier, Amsterdam 2006.

[5] A.P. Râmbu, G.I. Rusu, *Superlattices Microstruct.* **47**, 300 (2010).

[6] Y.G. Wang, *J. Appl. Phys.* **44**, 354 (2003).

[7] G.G. Rusu, A.P. Rambu, M. Rusu, *J. Optoelectron Adv. Mater.* **10**, 339 (2008).

[8] Sunglac Cho, *Appl. Phys. Lett.* **75**, 2761 (1999).

[9] *Polycrystalline and Amorphous Thin Films and Devices*, Ed. L.L. Kazmerski, Academic Press, New York 1980.

[10] S.W. Xue, X.T. Zu, W.L. Zhou, H.X. Deng, X. Xiang, L. Zhang, H. Deng, *J. Alloys Comp.* **448**, 21 (2008).

[11] E.K. Kim, S. Kim, *Superlattices Microstruct.* **42**, 343 (2007).

[12] P. Bhattacharya, R.R. Das, R.S. Katiyar, *Thin Solid Films* **564**, 447 (2004).

[13] K.L. Chopra, *Thin Film Phenomena*, McGraw-Hill, New York 1969.

[14] Z.W. Li, W. Gao, R.J. Reeves, *Surf. Coat. Technol.* **198**, 319 (2005).

[15] E.S. Tuzemen, S. Eker, H. Kavak, R. Esen, *Appl. Surf. Sci.* **255**, 6195 (2009).

[16] Q.P. Wang, X.J. Zhang, C.Q. Wang, S.H. Chen, X.H. Wu, H.L. Ma, *Appl. Surf. Sci.* **254**, 5100 (2008).

[17] K.C. Kim, E.K. Kim, Y.S. Kim, *Superlattices Microstruct.* **42**, 246 (2007).

[18] G.G. Rusu, M. Rusu, *Solid State Commun.* **M6**, 363 (2000).

[19] G.I. Rusu, M.E. Popa, G.G. Rusu, I. Salaoru, *Appl. Surf. Sci.* **218**, 222 (2003).

[20] B.D. Cullity, *Elements of X-ray Diffraction*, Addison--Wesley, Reading, Massachusetts 1978, p. 356.

[21] *American Standard for Testing Materials*, X-ray Powder Diffraction Data, File Card 5-0664.

[22] J.N. Pankove, *Optical Processes in Semiconductors*, Dover, New York 1971.

[23] G.I. Rusu, M. Diciu, C. Pirghie, M.E. Popa, *Appl. Surf. Sci.* **253**, 9500 (2007).

[24] T. Yamamoto, T. Shiosaki, A. Kawabata, *J. Appl. Phys.* **51**, 3113 (1980).

[25] H. Metin, R. Esen, *Semicond. Sci. Technol.* **18**, 647 (2003).

[26] S.J. Pearton, D.P. Norton, I.Y. Heo, T. Steiner, *J. Vac. Sci. Technol. B* **22**, 155504 (2004).

[27] C.S. Barret, F.B. Massalski, *Structure of Metals*, Pergamon Press, Oxford 1980.

[28] J. Tauc, R. Grigorovici, Y. Vancu, *Phys. Status Solidi* **15**, 627 (1966).

[29] J. Mass, P. Bhattacharya, R.S. Katiyar, *Mater Sci. Eng. B* **9**, 103 (2003).

[30] J. Benn, P.R. Manyon, V.K. Vaedyan, *Bull. Mater. Sci.* **28**, 487 (2005).

[31] H.C. Ong, A.X.E. Zhu, G.T. Du, *Appl. Phys. Lett.* **80**, 941 (2002).

[32] C. Wang, P. Zhang, J. Yue, Y. Zhang, L. Zheng, *Physica B* **403**, 2235 (2008).

[33] M. Smirnov, C. Baban, G.I. Rusu, *Appl. Surf. Sci.* **256**, 2405 (2010).

[34] J.K. Furdina, *J. Appl. Phys.* **64**, 29 (1988).